Towards improved drug action : target binding kinetics and functional efficacy at the mGlu2 receptor

Doornbos, M.L.J.

CHAPTER 2

Molecular mechanism of positive allosteric modulation of the metabotropic glutamate receptor 2 by JNJ-46281222

Maarten L J Doornbos, Laura Pérez-Benito, Gary Tresadern, Thea Mulder-Krieger, Ilse Biesmans, Andrés A Trabanco, Jose María Cid, Hilde Lavreysen, Adriaan P IJzerman & Laura H Heitman

British Journal of Pharmacology 173 (2016) 588–600. doi:10.1111/bph.13390

2

ABSTRACT

Background and purpose:

Allosteric modulation of the $mGlu_2$ receptor is a potential strategy for treatment of various neurological and psychiatric disorders. Here we describe the *in vitro* characterization of the $mGlu_2$ PAM JNJ-46281222 and its radiolabelled counterpart [^{3}H]JNJ-46281222. Using this novel tool, we also describe the allosteric effect of orthosteric glutamate binding and the presence of a bound G protein on PAM binding and use computational approaches to further investigate the binding mode.

Experimental approach:

We have used radioligand binding studies, functional assays, site-directed mutagenesis, homology modelling and molecular dynamics to study the binding of JNJ-46281222.

Key results:

JNJ-46281222 is an $mGlu_2$-selective, highly potent PAM with nanomolar affinity (K_D = 1.7 nM). Binding of [^{3}H]JNJ-46281222 was increased by the presence of glutamate and greatly reduced by the presence of GTP, indicating the preference for a G protein bound state of the receptor for PAM binding. Its allosteric binding site was visualized and analysed by a computational docking and molecular dynamics study. The simulations revealed amino acid movements in regions expected to be important for activation. The binding mode was supported by [^{3}H]JNJ-46281222 binding experiments on mutant receptors.

Conclusion and implications:

Our results obtained with JNJ-46281222 in unlabelled and tritiated form further contribute to our understanding of $mGlu_2$ allosteric modulation. The computational simulations and mutagenesis provide a plausible binding mode with indications of how the ligand permits allosteric activation. This study is therefore of interest for $mGlu_2$ and class C receptor drug discovery.

INTRODUCTION

The metabotropic glutamate (mGlu) receptors modulate cell excitability and synaptic transmission when activated by endogenous glutamate. They belong to the glutamate-like subfamily (class C) of G protein-coupled receptors (GPCRs) and are divided into three subgroups, Group I ($mGlu_{1, 5}$), Group II ($mGlu_{2, 3}$) and Group III ($mGlu_{4, 6-8}$), based on their sequence homology, second messenger coupling and pharmacology.[1,2]

Structurally, class C GPCRs are characterized by a large extracellular orthosteric binding domain, the so called Venus Flytrap Domain (VFT), which is connected to the seven transmembrane (7TM) domain by a cysteine-rich domain (CRD).[3,4] They are obligatory dimers and mainly exist as homodimers linked by a disulfide bond in the VFT.[5,6]

Activation of the $mGlu_2$ receptor is a potential strategy for the treatment of psychiatric disorders such as schizophrenia, anxiety and depression.[7] Interestingly, $mGlu_2$ receptor activation can be enhanced by positive allosteric modulators (PAMs), which have little or no intrinsic efficacy and enlarge the effect exerted by endogenously released glutamate.[8] The orthosteric binding site is highly conserved between mGlu receptors and it is thus hard to develop selective orthosteric ligands. Next to that, allosteric ligands are more capable of crossing the blood brain barrier as they are less polar, due to their binding in the more hydrophobic 7TM domain.[9] For these reasons the number of PAMs described has increased tremendously over the last decade.[10] These include compounds such as LY487379[11], BINA[12], THIIC (also known as LY2607540)[13] and JNJ-40068782[14], which have been extensively characterized both *in vitro* and *in vivo*. Importantly, two $mGlu_2$ PAMs have reached clinical trials so far. Development of AZD8529 (described in patent WO2008150233)[15] from AstraZeneca was discontinued after a Phase 2a study in schizophrenic patients due to a lack of efficacy.[16] JNJ-40411813 (also known as ADX71149) from Janssen Pharmaceuticals and Addex Therapeutics failed to meet the criterion for efficacy signal in patients with major depressive disorder with significant anxiety symptoms. In contrast, in an exploratory Phase 2a study in schizophrenia, not powered to determine statistical significance of effects rather a signal generation study, JNJ-40411813 met the primary objectives of safety and tolerability and also demonstrated an effect in patients with residual negative symptoms.[17]

The $mGlu_2$ allosteric binding pocket has been elucidated by mutagenesis studies, which revealed an overlap between PAM and negative allosteric modulator (NAM) binding sites.[18–22] The recent crystallization of the first Class C GPCRs $mGlu_1$ and $mGlu_5$ 7TM in complex with NAM molecules enables accurate mGlu homology modelling.[23,24]

Here, the *in vitro* properties of JNJ-46281222 are described and we characterize [^{3}H]JNJ-46281222 as a high affinity $mGlu_2$ PAM. Its binding was studied in order to gain a better understanding of the relation between orthosteric and allosteric binding sites at the $mGlu_2$ receptor. In addition, molecular dynamics simulations based on an active state 7TM $mGlu_2$ receptor model were performed to analyse the binding mode of JNJ-46281222, which was validated experimentally in subsequent mutagenesis experiments. Altogether this work offers new insights into the functioning of the $mGlu_2$ receptor, which might contribute to development of new and improved PAMs.

METHODS

Chemicals and reagents

BINA, THIIC (a.k.a. LY2607540), RO4491533[25], AZD8529, JNJ-40068782, JNJ-46281222 (Fig. 1)[26] and [^{3}H]JNJ-46281222 were synthesized at Janssen Research and Development. DCG-IV was purchased at R&D systems Europe (Abingdon, United Kingdom). [^{3}H]DCG-IV and [^{3}H]LY341495 were obtained from American Radiolabeled Companies (St. Louis, MO, USA). GTP and glutamate were purchased from Sigma-Aldrich (St. Louis, MO, USA). Chinese hamster ovary cells (CHO-K1, ATCC: CCL-61) were from ATCC (Rockville, MD, USA). Other chemicals were from standard commercial sources.

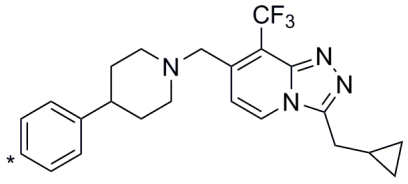

Figure 1. Chemical structure of JNJ-46281222. The position of the tritium label in [^{3}H]JNJ-46281222 is denoted by *.

Tritiation of JNJ-46281222

A solution of triethylamine (110μL) in ethanol (5 mL) was prepared. From this solution 0.2 mL was added to a tritiation reaction vial which contained the brominated precursor 7-((4-(4-bromophenyl)piperidin-1-yl)methyl)-3-(cyclopropylmethyl)-8-(trifluoromethyl)-[1,2,4]triazolo[4,3-a]pyridine (1.9 mg) and palladium on carbon (10%, 1.9 mg). The reaction mixture was attached to a tritium manifold (RC Tritec, Teufen, Switzerland) and degassed. Next tritium gas was placed on top of the reaction mixture (approximately 180 mbar) and was stirred for 8 minutes at room temperature. The remaining tritium gas was trapped on a uranium bed and all volatile compounds were lyophilized to a waste ampoule. The crude reaction mixture was rinsed with methanol (3x150 μL), dissolved in ethanol

(4x1mL), and filtered over an Acrodisc filter, yielding 2.04 GBq crude material. A portion (0.5 GBq) of this material was further purified and analyzed by high-performance liquid chromatography to obtain 0.36 GBq tritiated compound 7-((4-(4-tritiumphenyl)piperidin-1-yl)methyl)-3-(cyclopropylmethyl)-8-(trifluoromethyl)-[1,2,4]triazolo[4,3-a]pyridine (radiochemical purity of 97.4%; specific activity of 25 Ci/mmol).

Cell Culture

CHO-K1 cells stably expressing the wildtype (WT) $hmGlu_2$ receptor (CHO-K1_$hmGlu_2$) were grown in Dulbecco's modified Eagle's medium (DMEM) supplemented with 10% (v/v) fetal calf serum, 88 IU·mL^{-1} penicillin, 88 μg·mL^{-1} streptomycin, 30.5 μg·mL^{-1} L-proline and 400 μg·mL^{-1} G418 at 37°C and 5% CO_2. CHO-K1 cells were cultured in the same medium without G418. Cells were subcultured at a ratio of 1:10 twice every week.

Cell Membrane Preparation

CHO-K1_$hmGlu_2$ cells were plated into 15 cm Ø plates in DMEM without G418. When cells were grown to 70% confluency sodium butyrate (final concentration 5 mM) was added to the plates.[27] After 24 hours cells were detached from the plates by scraping them into 5 ml of PBS and subsequently centrifuged for 5 min at 1500 rpm. The pellets were resuspended into ice-cold Tris buffer (50 mM Tris-HCl pH 7.4) and homogenized using an Ultra Turrax homogenizer (IKA-Werke GmbH & Co.KG, Staufen, Germany). Membranes and the cytosolic fraction were separated by centrifugation at 31,000 rpm in an Optima LE-80 K ultracentrifuge (Beckman Coulter, Fullerton, CA) at 4°C for 20 min. Pellets were resuspended in 10 ml Tris buffer and the centrifugation and homogenization steps were repeated. The remaining pellets were suspended into assay buffer (50 mM Tris-HCl pH 7.4, 2 mM $CaCl_2$, 10 mM $MgCl_2$) and the homogenization step was repeated. Aliquots of membrane suspension were stored at -80°C. Membrane protein concentrations were determined using a BCA protein determination.[28]

Transient Transfection

Transient transfections were performed as previously described.[22]

Western blot analysis

$hmGlu_2$ receptor membrane samples were thawed and homogenized using an Ultra Turrax homogenizer at 24,000 rpm. For each membrane suspension sample 200 μl was transferred to an eppendorf tube and 400 μl of RIPA buffer (150 mM NaCl, 1.0% IGEPAL® CA-630, 0.5% sodium deoxycholate, 0.1% SDS, 50 mM Tris, pH 8.0, Sigma-Aldrich) complemented with phosphatase and protease inhibitors (Roche, Basel, Switzerland) was added. Homogenates were incubated for 30 min on ice and centrifuged at 14,000 rpm (20 min, 4°C). The supernatants were collected and protein concentrations were determined using the BCA method

(Smith et al., 1985). Samples were diluted with RIPA buffer (0.15 μg/ml) and denatured by LDS sample buffer and reducing agent (Life Technologies, Invitrogen, Carlsbad, CA, USA) (final concentration 0.1 μg/ml). The membrane protein samples were electrophoresed (3 μg), using an 18-well 4-12% polyacrylamide gel (Bio-Rad, Hercules, CA, USA) at 90-160V. The proteins on the gels were then electroblotted onto a Trans blot turbo 0.2 μm nitrocellulose membrane (Bio-Rad), by using a Trans-blot Turbo transfer system (Bio-Rad). Membranes were blocked for 1 hour at room temperature in Tween-20 Tris-buffered Saline (TBS-T: 10 mM Tris-HCl pH 8.0, 150 mM NaCl, 0.05% Tween-20) containing 5% non-fat dry milk (Santa Cruz Biotechnology, Dallas, TX, USA), and incubated with the primary antibody overnight at 4 °C allowing gentle shaking at a final concentration of 0.75 μg/ml (specific monoclonal mouse anti-hmGlu2 antibody, Abcam ab15672, Cambride, United Kingdom). Blots were washed five times with TBS-T buffer and incubated with the secondary antibody for 1h at room temperature (polyclonal HRP-linked sheep anti-mouse IgG whole antibody, GE healthcare, little Chalfont Buckinghamshire, United Kingdom). Immunostaining was revealed after washing with TBST buffer via SuperSignal West Dura Extended Duration Substrate (Thermo scientific, Cramlington, United Kingdom). Signals were captured and quantified by chemiluminescence (G-box Syngene, Syngene, Cambridge, United Kingdom). For reprobing, membranes were stripped of using Restore™ Western Blot Stripping Buffer (Thermo scientific) for 15 min with agitation at room temperature. Before incubation with anti actin antibody (Millipore, Billerica, CA, USA, MAB1501, dilution 1:10000), the membranes were washed 3 times (5 min) in TBS-T and blocked 1h in 5% non-fat dry milk.

Radioligand binding assays

[^{3}H]JNJ-46281222 Binding

After thawing, membranes were homogenized using an Ultra Turrax homogenizer at 24,000 rpm. Samples were diluted in ice-cold assay buffer (50 mM Tris-HCl pH 7.4, 2 mM $CaCl_2$, 10 mM $MgCl_2$) to a total reaction volume of 100 μl and incubated at 15°C. Nonspecific binding was determined using 10 μM JNJ-40068782, DMSO concentrations were ≤0.25%.

For saturation experiments CHO-K1_hmGlu$_2$ membrane aliquots, containing 30 μg protein, and nine increasing concentrations of radioligand, ranging from 0.4 to 20 nM, were incubated for 60 minutes to allow equilibrium to be reached for all concentrations of radioligand. Nonspecific binding was determined at three concentrations of radioligand.

Association experiments were carried out by incubation of 6 nM of radioligand and membrane aliquots, containing 20 or 30 μg of protein for assays in presence or absence of 1 mM glutamate, respectively. The amount of receptor-bound radioligand was determined at different time points up to 180 minutes.

Dissociation experiments were performed by a 60 minute pre-incubation of 6 nM radioligand and membrane aliquots containing 30 μg protein or for assays in the presence of 1 mM glutamate or GTP, 20 or 50 μg respectively. Dissociation was initiated by addition of 10 μM

JNJ-40068782 (final concentration) in 5 µl. and the amount of remaining receptor-bound radioligand was determined at different time points up to 120 minutes.

Displacement experiments were performed using 6 nM of radioligand and 10 concentrations of competing ligand, diluted by an HP D300 digital dispenser (Tecan, Giessen, The Netherlands) and incubated for 60 minutes. Membrane protein aliquots containing 30 or 40 µg were used for membranes stably expressing the $hmGlu_2$ receptor or for transiently transfected $hmGlu_2$ receptor constructs, respectively.

For all assays, incubation was terminated by rapid filtration over GF/C filters through a Brandel harvester 24 (Brandel, Gaithersburg, MD, USA) or over GF/C filterplates (PerkinElmer, Groningen, The Netherlands) on a PerkinElmer filtermate harvester. Filters were subsequently washed at least three times using ice-cold wash buffer (50 mM TRIS-HCl pH 7.4). Filter-bound radioactivity was determined using liquid scintillation spectrometry on a TRI-Carb 2810 TR counter (PerkinElmer) or a P-E 1450 Microbeta Wallac Trilux scintillation counter (PerkinElmer). [^{3}H]JNJ-46281222 did not bind to CHO-K1 membranes without $hmGlu_2$ receptor expression (data not shown). For all radioligand binding experiments, radioligand concentrations were chosen such that <10% of the amount added was receptor-bound.

[^{3}H]LY341495 Binding

For saturation experiments, various concentrations of [^{3}H]LY341495 from 0.5 to 30 nM were incubated with 10 µg membrane protein from the same batch of membranes as used for [^{3}H]JNJ-46281222 saturation binding experiments at 15°C for 60 minutes in a total volume of 100 µl. Nonspecific binding was determined at three concentrations of radioligand in the presence of 1 mM glutamate. Incubations were terminated and samples obtained and analysed as described under '*[^{3}H]JNJ-46281222 Binding*'.

[^{3}H]DCG-IV Binding

For saturation experiments, unlabelled DCG-IV was spiked with 20% [^{3}H]DCG-IV, resulting in final concentrations from 50 to 1500 nM. DCG-IV was incubated with 75 µg membrane protein from the same batch of membranes as used for [^{3}H]JNJ-46281222 saturation binding experiments at 15°C for 60 minutes in a total volume of 100 µl. Nonspecific binding was determined at three concentrations of radioligand in presence of 10 µM LY341495. Incubations were terminated and samples obtained and analysed as described under '*[^{3}H]JNJ-46281222 Binding*'.

[^{35}S]GTPγS Binding

[^{35}S]GTPγS binding experiments were performed as previously described.[14]

Data analysis

Data analyses were performed using Prism 5.00 (GraphPad software, San Diego, CA, USA). K_D and B_{max} were determined by a saturation binding analysis, using the equation $Y = B_{max} \times K_D / (K_D + X)$. pIC_{50} values were obtained using non-linear regression curve fitting into a sigmoidal concentration-response curve using the equation: Y=Bottom + (Top-Bottom)/(1+10$^{(X-LogIC50)}$). pK_i values were obtained from pIC_{50} values using the Cheng-Prusoff equation.[29] Dissociation rate constants k_{off} were determined by using an exponential decay analysis of radioligand binding. Association rate constants k_{on} were determined using the equation $k_{on} = (k_{obs} - k_{off})/[L]$, in which L is the concentration of radioligand used for association experiments and k_{obs} is determined using exponential association analysis. Data shown are the mean ± SEM of at least three individual experiments performed in duplicate, unless stated otherwise. Statistical analysis was performed if indicated, using a two-tailed unpaired Student's t-test or one-way ANOVA with Dunnett's post-test. Observed differences were considered statistically significant if p-values were below 0.05.

Building an $mGlu_2$ receptor homology model

An active state model of the 7TM domain of human $mGlu_2$ receptor (Uniprot code Q14416) bound to G protein was built using a combination of structural templates. The crystal structure of the human $mGlu_5$ (PDB 4OO9)[24] was used to model all 7TM helices except TM6. Extracellular loop 2 (ECL2) is not refined in the $mGlu_5$ X-ray structure therefore this important loop was modelled based on the $mGlu_1$ receptor crystal structure (PDB 4OR2).[23] Finally, the β_2AR (PDB ID 3SN6)[30] active structure was used to model both TM6 in its distinct open conformation as well as the corresponding G protein. This monomer 7TM has been shown experimentally to be activated upon PAM binding[31] The sequence identity between $mGlu_2$ and $mGlu_5$ 7TM's was 51%. The initial model was constructed in MOE v2014.9 (Chemical computing group Inc., Montreal, QC, Canada) and then Maestro (Schrodinger LLC, New York, NY, USA) was used for structure preparation. The Protein Preparation tool was used to fix any missing sidechains/atoms, PROPKA assigned protonation states, the hydrogen bonding network was optimized, and brief minimisation to RMSD 0.5 Å was applied to remove any structural clashes. Amino acid numbering is based on recent recommendations.[32]

Docking of JNJ-46281222

The ligand was prepared for docking using Maestro. Its basic pK_a value was measured experimentally as 6.6. The structure activity relationship (SAR) of molecules from this series does not require a charged centre for $mGlu_2$ PAM activity.[33] Hence, JNJ-46281222 was modelled in an unionised state. Conformational sampling was performed with ConfGen and multiple conformers were docked into the $mGlu_2$ active state model using Glide XP. The docking grid was centered on the ligand position in the $mGlu_1$ receptor structure. Sampling was increased

in the Glide docking by turning on expanded sampling and passing 100 initial poses to post-docking minimisation. All other docking parameters were set to the defaults.

Molecular Dynamics Simulations

Molecular dynamics (MD) simulations were performed with GROMACS v4.6.5.[34] Ligand-receptor complexes were embedded in a pre-equilibrated box (10x10x19 nm) containing a lipid bilayer (297 POPC molecules) with explicit solvent (~47000 waters) and 0.15 M concentration of Na^+ and Cl^- (~490 ions). The total size of the system was 174000 atoms. Each system was energy minimized and subjected to a 5 step MD equilibration of 10, 5, 2, 2 and 2 ns respectively. In the first step the whole system was fixed except for the hydrogens. In the second, the protein loops were released from restraints. In the final three steps the restraints on the ligand and proteins were relaxed from 100, 50 and 10 $kJ.mol^{-1}nm^{-2}$ respectively. Production simulations were performed for time periods between 200 and 500 ns without restraints using a 2 fs time step. Constant temperature of 300K using separate v-rescale thermostats for Protein-Ligand, lipids, and water plus ions was used. The LINCS algorithm was applied to freeze bond lengths. Lennard-Jones interactions were computed using a 10 Å cut-off, and the electrostatic interactions were treated using PME also with a 10 Å cut-off. The AMBER99SD-ILDN force field[35] was used for the protein, the parameters described by Berger *et al.* (1997)[36] for lipids, and the general Amber force field (GAFF) and HF/6-31G*-derived RESP atomic charges for the ligand. This combination of protein and lipid parameters has recently been validated.[37]

RESULTS

Characterization of [^{3}H]JNJ-46281222

Firstly, the affinity of [^{3}H]JNJ-46281222 for the $mGlu_2$ receptor was determined by performing saturation binding experiments on membranes of CHO-K1 cells stably expressing the $hmGlu_2$ receptor (Fig. 2A). Receptor binding was saturable and defined by a K_D of 1.7 nM with a B_{max} of 1.1 pmol/mg protein. Homologous displacement experiments with [^{3}H]JNJ-46281222 resulted in a pK_i value of 8.33 for JNJ-46281222. In addition, a series of reference PAMs and a NAM based on various chemical scaffolds fully displaced [^{3}H]JNJ-46281222 binding, resulting in pK_i values ranging from 6.43 to 8.09 (Table 1), while pseudo-Hill coefficients were all close to unity. Secondly, kinetic association and dissociation experiments were performed to determine the association (k_{on}) and dissociation (k_{off}) rate constants (Fig. 2B; Table 2). Equilibrium binding of [^{3}H]JNJ-46281222 was reached within 30 minutes as assessed by kinetic association experiments and best fit with a one-phase model, whereas the dissociation curve was best fit with a two-phase model. This resulted in a k_{obs} value of 0.24 min^{-1} describing the association

and two values describing the dissociation, i.e. a $k_{off,1}$ value of 0.040 min^{-1} and a $k_{off,2}$ value of 0.77 min^{-1}.

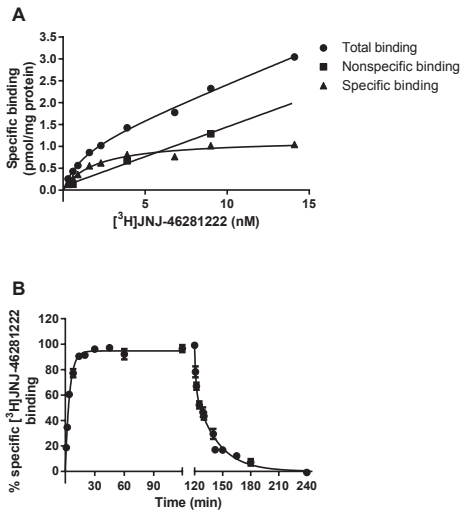

Figure 2. Characterization of [^{3}H]JNJ-46281222 binding to $mGlu_2$ receptors stably expressed at CHO-K1 membranes.
(A) Saturation analysis of [^{3}H]JNJ-46281222 binding. A representative experiment is shown with similar data being obtained in two additional experiments.
(B) Association and dissociation kinetics of 6 nM [^{3}H]JNJ-46281222 at the $mGlu_2$ receptor at 15°C. Association data was best fitted using a one-phase exponential association model, whereas data for dissociation curves were best fitted using a two-phase exponential decay model. Data are expressed as percentage of specific [^{3}H]JNJ-46281222 binding and are shown as mean ± SEM of at least four individual experiments. Where bars are not shown SEM values are within the symbol.

Table 1. Receptor affinity of $mGlu_2$ allosteric modulators determined by [^{3}H]JNJ-46281222 displacement experiments.

Compound	pK_i
JNJ-46281222	8.33 ± 0.14
JNJ-40068782	7.58 ± 0.08
BINA	7.22 ± 0.15
THIIC	7.10 ± 0.04
AZD8529	6.43 ± 0.03
RO4491533	8.09 ± 0.09

Data are shown as mean ± SEM of at least three individual experiments performed in duplicate.

Table 2. Kinetic binding parameters for [^{3}H]JNJ-46281222 binding to human $mGlu_2$ receptors in absence or presence of 1 mM glutamate.

	k_{obs} (min^{-1})	k_{on} ($nM^{-1}.min^{-1}$)[a]	k_{off} (min^{-1})[b]		K_D (nM)[c]
			$k_{off,1}$	$k_{off,2}$	
[^{3}H]JNJ-46281222	0.24 ± 0.019	-	0.040 ± 0.0061	0.77 ± 0.18	-
[^{3}H]JNJ-46281222 + 1 mM glutamate	0.19 ± 0.031	0.019 ± 0.0051	0.070 ± 0.0056	-	3.6 ± 0.99

Data are shown as mean ± SEM of at least three individual experiments performed in duplicate. [a] k_{on} was determined using the formula $k_{on} = (k_{obs} - k_{off})/[L]$. [b] All parameters were determined by computer analysis using a one-phase model, except for dissociation of [^{3}H]JNJ-46281222 in absence of glutamate which was best described by a two-phase model. [c] K_D was determined as the ratio k_{off} / k_{on}.

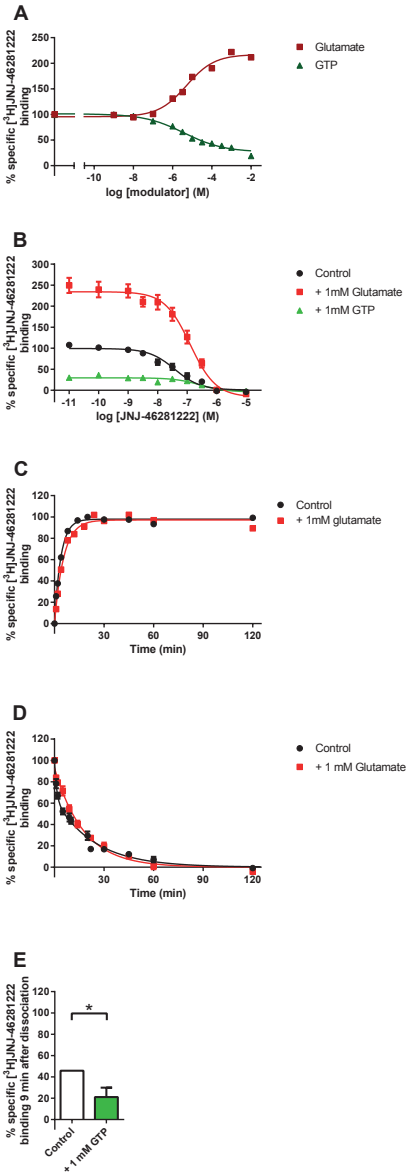

The effect of glutamate on [^{3}H]JNJ-46281222 binding to the mGlu$_2$ receptor

Increasing concentrations of glutamate enhanced [^{3}H]JNJ-46281222 binding by more than 2-fold (Fig. 3A; Table 3) with a modulatory potency (pEC_{50}) for glutamate of 5.27. [^{3}H]JNJ-46281222 displacement assays in the absence or presence of glutamate were performed with JNJ-46281222 and JNJ-40068782, which did not result in a significant change in affinity for both compounds (Fig. 3B; Table 4).

In addition, saturation binding of [^{3}H]JNJ-46281222 in the absence or presence of glutamate was performed (Fig. 4A), showing that the number of mGlu$_2$ PAM binding sites (B_{max}) was increased more than 2-fold in the presence of 1 mM glutamate, whereas the affinity (K_D) was not significantly affected (Table 5).

Next, the effect of glutamate on the kinetic association and dissociation rates of [^{3}H]JNJ-46281222 was examined. Glutamate decreased both rate constants to a small non-significant extent (Fig. 3C and 3D, Table 2). Moreover, whereas dissociation in the absence of glutamate was best described using a two-phase model, dissociation in the presence of 1 mM glutamate was best described with a one-phase model, with a k_{off} value of 0.070 min^{-1}. This presence of glutamate enabled further determination of the association rate constant k_{on}, which was 0.019 nM^{-1} min^{-1}. Based on these

Figure 3. The effects of glutamate and GTP on [^{3}H]JNJ-46281222 binding. (A) Increasing concentrations of glutamate enhance the specific binding of 6 nM [^{3}H]JNJ-46281222 to mGlu$_2$ receptors expressed at CHO-K1 cell membranes, whereas GTP inhibits specific [^{3}H]JNJ-46281222 binding. (B) Effects of glutamate and GTP on homologous displacement of [^{3}H]JNJ-46281222 from mGlu$_2$ receptors expressed at CHO-K1 membranes. Data are normalized to specific binding in absence of glutamate or GTP (set at 100%). (C, D) The effect of glutamate on mGlu$_2$ receptor association and dissociation of [^{3}H]JNJ-46281222. Data are expressed as specific binding of the respective curve, association plateaus are fixed at 100% specific [^{3}H]JNJ-46281222 binding, dissociation plateau fixed at 0% specific [^{3}H]JNJ-46281222 binding. (E) Specific [^{3}H]JNJ-46281222 binding after nine minutes of dissociation in absence or presence of GTP. * p-value <0.05 versus control, determined using a two-tailed unpaired Student's t-test. All graphs are shown as mean ± SEM of three to six individual experiments performed in duplicate. Where bars are not shown SEM values are within the symbol.

kinetic parameters, the kinetic K_D was determined according to the equation $K_D = k_{off} / k_{on}$, resulting in a K_D value of 3.6 nM for [^{3}H]JNJ-46281222 in the presence of glutamate (Table 2), which was in good agreement with the K_D value obtained from saturation experiments.

Table 3. Pharmacological characterization of the effects of glutamate or GTP on specific [^{3}H]JNJ-46281222 binding to mGlu$_2$ receptors.

	pEC_{50} / pIC_{50}	E_{max} (%)[a]	Hill slope
Glutamate	5.27 ± 0.08	125 ± 9.0	0.49 ± 0.04
GTP	5.95 ± 0.21	-65 ± 8.0	-0.58 ± 0.03

Data are shown as mean ± SEM of three individual experiments performed in duplicate. [a] E_{max} was determined as difference in total specific binding compared to binding in absence of glutamate or GTP (set at 100%).

The effect of GTP on [^{3}H]JNJ-46281222 binding to the mGlu$_2$ receptor

Radioligand displacement assays in the presence of increasing GTP concentrations were performed to evaluate the importance of the presence of a bound G protein for [^{3}H]JNJ-46281222 binding. As depicted in Figure 3A, GTP inhibits [^{3}H]JNJ-46281222 binding by 65% with a pIC_{50} value of 5.95. The affinity of JNJ-46281222 was significantly decreased in the presence of 1 mM GTP, whereas this was not the case for JNJ-40068782 (Table 4). Subsequently, the effect of 1 mM GTP on the dissociation rate of [^{3}H]JNJ-46281222 was examined. Since it was impossible to obtain reliable full curves with the vastly decreased [^{3}H]JNJ-46281222 window under these conditions, [^{3}H]JNJ-46281222 dissociation in the presence of 1 mM GTP was only determined at a single time point (i.e. after nine minutes) and compared to the extent of dissocation in the absence of GTP at that same time point (Fig. 3E). In the presence of 1 mM GTP the relative amount of [^{3}H]JNJ-46281222 still bound to the receptor after nine minutes was significantly lower than in its absence, indicating an increased dissociation rate.

Table 4. Displacement of [^{3}H]JNJ-46281222 by mGlu$_2$ PAMs JNJ-46281222 and JNJ-40068782 from human mGlu$_2$ receptors in absence (control) or presence of 1 mM glutamate or GTP.

	pIC_{50}			E_{max} (%)[a]	
	Control	+ 1mM Glu	+ 1mM GTP	+ 1mM Glu	+ 1mM GTP
JNJ-46281222	7.71 ± 0.17	7.63 ± 0.14	7.00 ± 0.16*	150 ± 24	-71 ± 4.4
JNJ-40068782	6.89 ± 0.06	7.15 ± 0.10	6.85 ± 0.06	127 ± 20	-77 ± 4.5

Data are shown as mean ± SEM of at least three individual experiments performed in duplicate. [a] Emax was determined as difference in total specific binding compared to binding in absence of glutamate or GTP (set at 100%). * p-value < 0.05 compared to pIC_{50} control, determined using one-way ANOVA with Dunnett's post-test.

Saturation binding of orthosteric radioligands to the mGlu$_2$ receptor

For comparison of the number of accesible orthosteric and allosteric binding sites, saturation experiments were performed using the orthosteric radioligands [^{3}H]DCG-IV and [^{3}H]LY341495 (Fig. 4B and 4C, Table 5). The mGlu$_2$ agonist [^{3}H]DCG-IV had a low affinity of 365 nM and a B_{max} value of 1.2 pmol/mg that corresponded to the B_{max} value of 1.1 pmol/mg

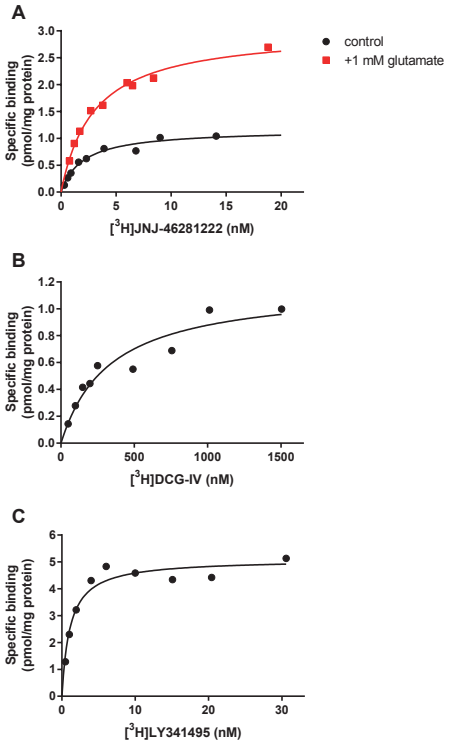

Figure 4. Saturation binding of radioligands to $mGlu_2$ receptors expressed at CHO-K1 membranes. (A) Saturation binding of [^{3}H]JNJ-46281222 to the $mGlu_2$ allosteric binding site in absence or presence of glutamate. (B) Saturation binding of [^{3}H]DCG-IV to the $mGlu_2$ orthosteric binding site, determined by "spiked" saturation (see text). (C) Saturation binding of [^{3}H]LY341495 to the orthosteric binding site. Graphs shown are from a representative experiment performed in duplicate in each case.

obtained for [^{3}H]JNJ-46281222. The high affinity antagonist [^{3}H]LY341495 had a K_D value of 2.4 nM and a B_{max} value of 5.1 pmol/mg, approximately 5-fold higher than for the PAM and for the agonist.

Quantification of potency of JNJ-46281222 at the $mGlu_2$ receptor

Figure 5A shows data from a representative determination of the concentration-effect curve of the glutamate-induced binding of [^{35}S]GTPγS in the absence and presence of various concentrations of JNJ-46281222; similar data were obtained in a second experiment. A 100 nM concentration of JNJ-46281222 enhanced the maximum glutamate-induced [^{35}S]GTPγS binding, i.e. glutamate's efficacy, by approximately 2-fold, shifting the curve upward, and increased the glutamate potency 5-fold, shifting the curve leftward. The potency of JNJ-46281222 was determined by quantifying the increase in response to a fixed EC_{20} glutamate concentration (4 μM), as depicted in Figure 5B. A pEC_{50} of 7.71 ± 0.02 was calculated while the maximal response, 193 ± 5%, was almost 2-fold higher compared to the maximal glutamate response exerted by 1 mM glutamate alone. In the absence of glutamate JNJ-46281222 shows a submaximal receptor activation of 42 ± 3% with a 10-fold lower pEC_{50} value of 6.75 ± 0.08.

Table 5. Characteristics of saturation binding of [^{3}H]JNJ-46281222 in absence or presence of glutamate, and the orthosteric radioligands [^{3}H]DCG-IV and [^{3}H]LY341495

Radioligand	K_D (nM)	B_{max} (pmol/mg protein)
[^{3}H]JNJ-46281222	1.7 ± 0.17	1.1 ± 0.12
+ 1 mM glutamate	2.5 ± 0.26	2.7 ± 0.25
[^{3}H]DCG-IV	330 / 400	1.1 / 1.2
[^{3}H]LY341495	2.4 ± 0.71	5.1 ± 0.39

Data for [^{3}H]JNJ-46281222 and [^{3}H]LY341495 are shown as mean ± SEM of at least three individual experiments performed in duplicate. The same parameters measured for [^{3}H]DCG-IV are from two independent experiments (values of both experiments are given).

Docking of JNJ-46281222 into the $mGlu_2$ 7TM Model

JNJ-46281222 was docked into the active state $mGlu_2$ homology model (Fig. 6A and 6B). The most energetically favourable binding pose is shown. The triazopyridine scaffold and lipophilic side chain substituent interact with the hydrophobic cluster formed between amino acids L639$^{3.32a.36c}$, F643$^{3.36a.40c}$, L732$^{5.43a.44c}$, W773$^{6.48a.50c}$ and F776$^{6.51a.53c}$. The cyclopropylmethyl substituent goes deepest into the receptor and interacts closely with F776$^{6.51a.53c}$. The hydrophobic residues cluster tightly around the triazopyridine scaffold with L639$^{3.32a.36c}$ and F643$^{3.36a.40c}$ interacting on one face of the scaffold and L732$^{5.43a.44c}$ and W773$^{6.48a.50c}$ on the other. Amino acid N735$^{5.47a.47c}$ acts as an H-bond donor to the nitrogen acceptor (2.0 Å) in the triazo ring of the scaffold. The sidechain of tryptophan W773$^{6.48a.50c}$, which is conserved in the mGlu receptors, points into the membrane in the same orientation as in the $mGlu_5$ inactive state 7TM crystal structure. The cyclopropyl group makes a steric interaction at 2.3 Å distance. The CF_3 group of the scaffold enters between TM3 and TM5 above N735$^{5.47a.47c}$, and interacts with S731$^{5.42a.43c}$. The 4-phenylpiperidine substituent is directed towards the extracellular side of the binding site and the distal phenyl sits between F623$^{2.61a.56c}$ and H723^{ECL2}. The predicted binding mode overlaps with the allosteric site in $mGlu_1$ whereas the $mGlu_5$ modulator goes deeper into the receptor (Fig. S1).

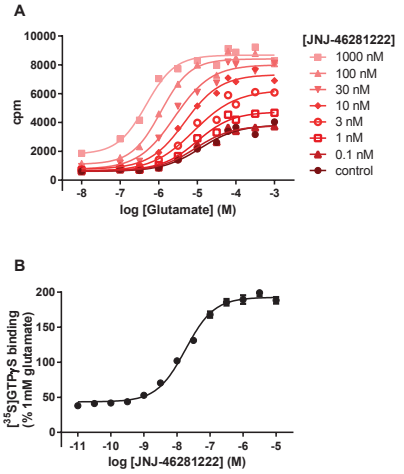

Figure 5. Characterization of potency of JNJ-46281222. (A) Stimulation of [^{35}S]GTPγS binding to $mGlu_2$ receptors induced by increasing concentrations of JNJ-46281222. A representative experiment is shown, with similar data obtained in a second experiment. Data are expressed as the percentage of maximal response induced by 1 mM glutamate. (B) Dose-response curve of JNJ-46281222 in presence of glutamate (EC_{20}, 4 μM) on the binding of [^{35}S]GTPγS binding. Data are expressed as the percentage of maximal response induced by 1 mM glutamate and are shown as mean ± SEM of thirteen individual experiments performed in triplicate. Where bars are not shown SEM values are within the symbol.

The location of the allosteric binding pocket of JNJ-46281222 at the $mGlu_2$ receptor

In order to validate the suggested location of the JNJ-46281222 binding site, radioligand binding assays were performed on transiently transfected $mGlu_2$ wild-type and mutant receptors. For the latter, mutations F643A$^{3.36a.40c}$ and N735D$^{5.47a.47c}$ were selected, since molecular docking studies indicated that these amino acids (amongst others) had important interactions with JNJ-46281222. Receptor expression was confirmed by Western blot analysis (Fig.7B). [^{3}H]JNJ-46281222 binding to the selected $mGlu_2$ receptor mutants, was significantly decreased by approximately 10-fold compared to WT, as shown in Figure 7A.

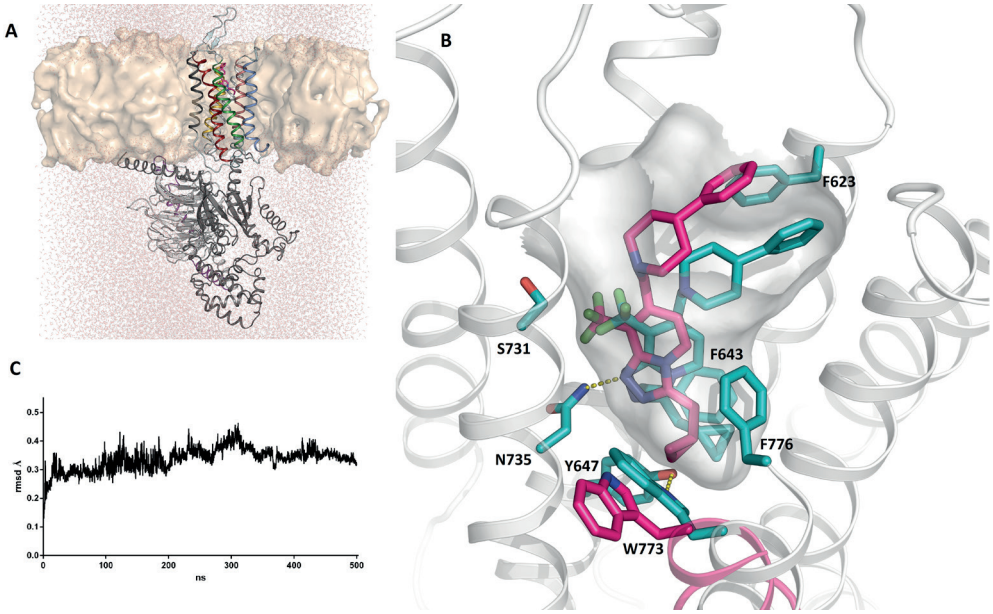

Figure 6. Molecular dynamics (MD) simulations of the binding of JNJ-46281222 to the $mGlu_2$ receptor. (A) The complete system used for MD simulations, including $mGlu_2$ receptor 7TM monomer, G protein, ligand (JNJ-46281222, magenta), lipids and solvent. (B) Close up of 7TM binding site showing interaction with a subset of important amino acids. MD starting position for ligand is coloured magenta; snapshot after 200 ns is turquoise. Movement of $W773^{6.48a.50c}$ from outwards orientation (magenta) at start of simulation to inwards orientation (turquoise) is highlighted. (C) RMSD of $mGlu_2$ receptor monomer during the simulation.

Molecular dynamics simulations of JNJ-46281222 and $mGlu_2$ 7TM Model

MD simulations of JNJ-46281222 docked in the WT active state $mGlu_2$ receptor model together with the G protein were performed for 500 ns. The overall structure was stable throughout the simulation with little fluctuation in RMSD of the 7TM (Fig. 6C). The G protein also showed little structural fluctuation and remained bound to the intracellular side of the receptor keeping TM6 in an open conformation. The ligand maintained key interactions with amino acids such as $L639^{3.32a.36c}$, $F643^{3.36a.40c}$ and $N735^{5.47a.47c}$ (Fig. 6B). Amino acids in the vicinity of JNJ-46281222 moved, and adopted alternative orientations which remained stable throughout the rest of the simulation. For instance, $W773^{6.48a.50c}$ made a large rotational movement inwards after 20 ns which was permitted by adjustment of the cyclopropylmethyl away from TM5 and towards $F643^{3.36a.40c}$. The tryptophan $W773^{6.48a.50c}$ then rotated into the 7TM binding site to maintain interaction with the ligand whilst forming a new H-bond interaction via its indole NH donor to the phenolic oxygen of $Y647^{3.39a.43c}$. Three additional replica simulations were performed for 200 ns using the same input but different starting velocities. Two of these showed consistent behaviour of $W773^{6.48a.50c}$. Additional MD simulations performed on the same system but without ligand did not display the inward rotation of $W773^{6.48a.50c}$. Likewise, the sidechain remained outwards during a separate simulation with ligand but

without G protein. Regarding the distal tail of JNJ-46281222, the phenyl moiety moved deeper into the 7TM binding site during the 500 ns simulation and continued to interact with F623$^{2.61a.56c}$ but no longer had contacts with H723 (mutation of which had previously shown no effect on JNJ-46281222 functional activity.)[22] Simulations performed on F643A$^{3.36a.40c}$ and N735D$^{5.47a.47c}$ mutant receptors were also stable with respect to the overall 7TM. However, for the N735D$^{5.47a.47c}$ mutant, the ligand made a significant departure from its starting orientation. In summary, the MD simulations revealed the predicted binding mode to be stable and consistent with amino acids making key interactions.

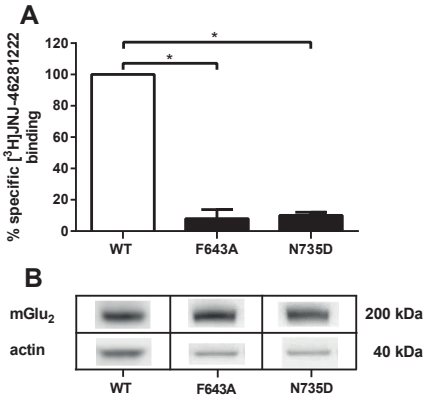

Figure 7. (A) Radioligand binding to $mGlu_2$ receptor mutants F643$^{3.36a.40c}$ and N735$^{5.47a.47c}$. Specific [^{3}H]JNJ-46281222 binding to WT or mutant $mGlu_2$ receptors, transiently transfected in CHO-K1 cells. Data were normalized to % specific binding compared to binding to WT $mGlu_2$ receptors and are expressed as mean ± SEM of three individual experiments performed in duplicate. (B) Representative immunoblot of WT (left panel) and mutant $mGlu_2$ receptors (middle, F643, and right, N735, panel) and actin. * p-value < 0.05 compared to WT, analysis was done using unnormalized data and determined using one-way repeated-measures ANOVA with Dunnett's post-test.

DISCUSSION

We describe JNJ-46281222 as a high affinity $mGlu_2$ PAM (K_D = 1.7 nM) with a high modulatory potency (pEC_{50} = 7.71 ± 0.02) on the effect of the endogenous agonist glutamate in a [^{35}S]GTPγS binding assay, where it increased glutamate's maximum effect by approximately 2-fold to its 'ceiling' allosteric effect.[38] These data are in line with previously reported affinity data for JNJ-46281222.[22] JNJ-46281222 on its own displayed a submaximal receptor activation of 43 ± 3% in the [^{35}S]GTPγS binding assay, with a potency (pEC_{50} = 6.75 ± 0.08) that is 10-fold lower compared to its potency to modulate glutamate activity. However, we prefer to refer to JNJ-46281222 as a PAM and not as a PAM-agonist for at least two reasons. First, we cannot fully rule out the presence of endogenous receptor-bound glutamate. Secondly, the cell line used has a high receptor density, potentially amplifying receptor responses. The potency and affinity of this PAM are higher than any other extensively reported $mGlu_2$ PAMs including JNJ-40068782 (Table 1).[10,14] In addition to its valuable properties for *in vitro* experiments,

[^{3}H]JNJ-46281222 can also be used for *ex vivo* $mGlu_2$ receptor occupancy studies, whereas this cannot be done with [^{3}H]JNJ-40068782.[39]

To investigate the relation between the orthosteric, allosteric and G protein binding sites, we performed [^{3}H]JNJ-46281222 binding experiments in the absence and presence of either glutamate or GTP. The observation by Lavreysen *et al.* (2013)[14] and Lundström *et al.* (2011)[21] - binding of an $mGlu_2$ PAM is enhanced in the presence of a high concentration of the orthosteric agonist glutamate - was taken as a starting point for our work. In our case, the total amount of sites accesible for JNJ-46281222 binding was significantly enlarged by approximately 2.5-fold by the addition of glutamate (Fig. 3B and 4A). This indicates a conformational change in receptor structure that increases the population of receptors in a more favourable state for PAM binding and recognition. In addition, we performed [^{3}H]JNJ-46281222 binding experiments in the presence of increasing concentrations of glutamate, confirming the increase in specific binding with a micromolar potency for glutamate (pEC_{50} = 5.27) and a pseudo-Hill slope of less than unity (n_H = 0.49), indicative of allosteric enhancement of JNJ-46281222 binding by the agonist. Thereby, this experiment clearly revealed two-way allosterism between orthosteric and allosteric binding sites.[40]

We showed that the presence of glutamate does not significantly change the affinity of $mGlu_2$ PAMs, as was observed previously for $mGlu_5$ PAMs.[41] Specifically, the affinity of JNJ-46281222 was not affected by the presence of glutamate, as both K_D values were similar (1.7 and 2.4 nM, Table 5), just like the pIC_{50} values of 7.71 and 7.63 (Table 4). For JNJ-40068782 we did not find a significant increase in affinity, as shown by the pIC_{50} values, whereas Lavreysen *et al.* (2013)[14] showed an increase in K_D values. This could be indicative for between membrane pool or between lab variations. The presence of glutamate decreased the rate of both association and dissociation of [^{3}H]JNJ-46281222 to a small non-significant extent. Most striking was the ability of glutamate to change the two-phasic character of dissociation towards a one-phase dissociation. In general, a two-phasic character can be explained by the presence of two binding sites, known as the high- and low affinity binding sites within a receptor population.[38] In this case, one could postulate that glutamate increases the number of PAM binding sites and fixes the receptor into a single conformational state resulting in a single dissociation rate.

Previous studies showed that binding of only one PAM per dimer is sufficient for enhancement of receptor activity.[42] It was hypothesized that upon receptor activation only one of the 7TM domains is turned on and activates a G protein.[43] Whereas these studies came to their conclusions using changes in the receptor structure, we evaluated the number of orthosteric and allosteric binding sites using radioligand saturation binding assays on the WT $mGlu_2$ receptor. Interestingly, saturation binding of the orthosteric agonist [^{3}H]DCG-IV revealed a B_{max} similar to [^{3}H]JNJ-46281222 (Table 5), indicating the same number of binding sites for

both orthosteric agonists and PAMs. So, whereas only one PAM per receptor dimer is necessary for efficacy,[43] it seems that two PAMs actually bind the receptor in the absence of glutamate. On the other hand, presence of glutamate increases the number of allosteric binding sites, as shown by the increased B_{max} of [^{3}H]JNJ-46281222 (Table 5). This indicates that addition of glutamate might lead to [^{3}H]JNJ-46281222 binding to both glutamate-bound and -unbound receptors. Interestingly, the increase in accesible PAM binding sites induced by the presence of glutamate was not seen the other way around. Both $mGlu_2$ PAMs JNJ-40068782 and JNJ-40411813 increased the affinity of [^{3}H]DCG-IV but not its B_{max} value.[14,39]

The presence of GTP decreased [^{3}H]JNJ-46281222 binding by 65%, indicating that PAM binding is dependent on the availability of receptors that are coupled to a G protein. Moreover, the pseudo-Hill coefficient of less than unity (n_H = -0.58), confirms an allosteric rather than competitive effect of GTP on JNJ-46281222 binding. The necessity of a coupled G protein for PAM binding was further confirmed by saturation binding experiments with [^{3}H]JNJ-46281222, the orthosteric agonist [^{3}H]DCG-IV and antagonist [^{3}H]LY341495, showing that approximately 5-fold more receptors are labeled by an antagonist than an agonist or PAM radioligand (Fig. 4, Table 5). Decades ago, the presence of GTP has already been shown to decrease agonist but not antagonist binding in class A GPCRs (e.g., Williams and Lefkowitz, 1977).[44] For the $mGlu_2$ receptor this was also shown for the orthosteric agonists DCG-IV and LY354740, where GTPγS decreased their binding up to 80% with nanomolar potency.[45,46] In our hands, in addition to a reduction of the total binding level, GTP also induced a significant decrease in binding affinity of JNJ-46281222, whereas it did not change the affinity of JNJ-40068782 (Table 4). These findings contribute to the idea that different PAMs can have different effects on the interplay between receptor binding sites. To our knowledge we are the first to describe the necessity for a G protein bound state of the receptor for PAM binding, as shown by the effects of GTP on the binding of [^{3}H]JNJ-46281222 to the $mGlu_2$ receptor.

Previous mutagenesis studies revealed the molecular determinants vital for $mGlu_2$ PAM functional activity.[18,19,22] However, PAM binding on mutant receptors has not been previously examined. Docking of JNJ-46281222 into the 7TM $mGlu_2$ receptor model revealed direct interactions with, amongst others, F643$^{3.36a.40c}$ and N735$^{5.47a.47c}$. In order to confirm the proposed binding pose of JNJ-46281222 within the $mGlu_2$ 7TM domain, we performed [^{3}H]JNJ-46281222 binding experiments to transiently transfected $mGlu_2$ receptor mutants F643A$^{3.36a.40c}$ and N735D$^{5.47a.47c}$. Their binding was reduced evenly and significantly compared to the transiently transfected WT $mGlu_2$ receptor, showing that these amino acid residues are vital for $mGlu_2$ PAM binding. Together, these results indicate that the loss in $mGlu_2$ PAM functional efficacy, exerted by $mGlu_2$ receptor mutants F643A$^{3.36a.40c}$ and N735D$^{5.47a.47c}$, is caused by a loss of receptor binding.

We have presented hypotheses for the overlap and possible binding mode of $mGlu_2$ PAMs.[22,47] Here we used MD simulations of JNJ-46281222 in an active state 7TM $mGlu_2$ model which confirmed the binding mode was stable throughout the simulation. We observed movement of $W773^{6.48a.50c}$ which is part of a WLAFxPI sequence on TM6 that is conserved across mGlu receptors. The sidechain rotated inwards and interacted with the ligand and $Y647^{3.39a.43c}$. The 6.48a.50c position is located on TM6 in the transmission switch for class A GPCRs.[48] Rotamer movements of this tryptophan in rhodopsin along with the kink induced by the neighbouring proline, contribute to the outward movement of TM6 to permit activation. Also, the movement of $W773^{6.48a.50c}$ to disturb H-bonding in the cluster of amino acids involving $Y647^{3.39a.43c}$ and the conserved water molecule may play a role in the functional activity of class C allosteric modulators.[24] This is just above the important region for Na^+ ion modulation of $A_{2A}AR$ receptors.[49] Finally, a recent report suggests activation of $mGlu_2$ dimers proceeds from inactive TM4/5-TM4/5 interaction to TM6-TM6 interaction in the active state.[50] It seems plausible that inward movement of large sidechains on TM6 will enable the rotation of the monomers to the active state. Further work is needed to provide a deeper understanding of the allosteric modulator action on this $mGlu_2$ monomer and the full length dimeric receptor.

In conclusion, we have characterized the selective and highly potent $mGlu_2$ PAM JNJ-46281222 and its corresponding radioligand [^{3}H]JNJ-46281222. Its characteristics make it the preferred PAM radioligand for studying the $mGlu_2$ receptor. The orthosteric agonist glutamate was shown to increase the number of PAM binding sites without affecting the affinity of JNJ-46281222. The necessity of a coupled G protein was shown by the fact that GTP induced a large decrease of PAM binding and that the number of PAM binding sites, like the orthosteric agonist, was much lower than the number of G protein independent antagonist binding sites. Both mutations $F643A^{3.36a.40c}$ and $N735D^{5.47a.47c}$ caused a large decrease in PAM binding, thereby experimentally confirming the binding site as determined from the modelling and molecular dynamics studies. Together, these results contribute to the understanding of the mechanism of PAM binding and effect, which will hopefully contribute to current and future $mGlu_2$ PAM drug discovery programs.

Supporting figure S1

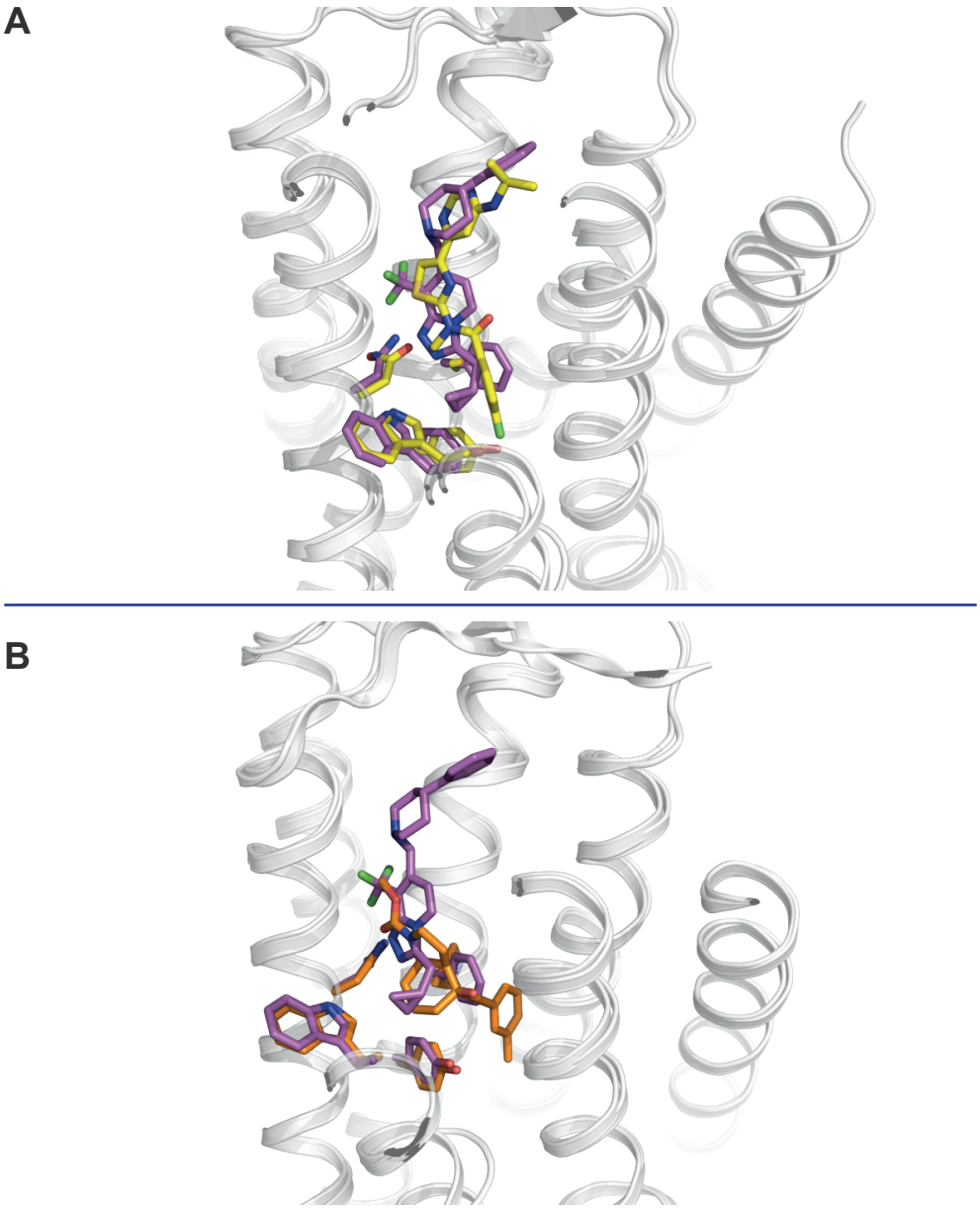

Figure S1. Comparison of the predicted JNJ-46281222 binding mode (purple) with that of NAMs in the $mGlu_1$ (A, yellow) and $mGlu_5$ (B, orange) receptor X-ray structures. A) $mGlu_1$ (yellow) compared to $mGlu_2$ model (purple). Position of allosteric ligand and selected amino acid side chains can be seen. mGlu1 X-ray structure is from PDB code 4OR2. B) $mGlu_5$ (orange) compared to $mGlu_2$ model (purple). Position of allosteric ligand and selected amino acid side chains can be seen. $mGlu_5$ X-ray structure is from PDB code 4OO9.

REFERENCES

1. Pin J-P, Duvoisin R. *Neuropharmacology*. **1995**; 34: 1–26.

2. Alexander SPH, Benson HE, Faccenda E, Pawson AJ, Sharman JL, Spedding M, Peters JA, Harmar AJ. *Br J Pharmacol*. **2013**; 170: 1459–581.

3. Muto T, Tsuchiya D, Morikawa K, Jingami H. *Proc Natl Acad Sci U S A*. **2007**; 104: 3759–64.

4. Niswender CM, Conn PJ. *Annu Rev Pharmacol Toxicol*. **2010**; 50: 295–322.

5. Romano C, Yang W-L, O'Malley KL. *J Biol Chem*. **1996**; 271: 28612–28616.

6. Kniazeff J, Prézeau L, Rondard P, Pin J-P, Goudet C. *Pharmacol Ther*. **2011**; 130: 9–25.

7. Nicoletti F, Bockaert J, Collingridge GL, Conn PJ, Ferraguti F, Schoepp DD, Wroblewski JT, Pin JP. *Neuropharmacology*. **2011**; 60: 1017–41.

8. Conn PJ, Christopoulos A, Lindsley CW. *Nat Rev Drug Discov*. **2009**; 8: 41–54.

9. Gregory KJ, Dong EN, Meiler J, Conn PJ. *Neuropharmacology*. **2011**; 60: 66–81.

10. Trabanco AA, Cid JM. *Expert Opin Ther Pat*. **2013**; 23: 629–47.

11. Johnson MP, Baez M, Jagdmann GE, Britton TC, Large TH, Callagaro DO, Tizzano JP, Monn JA, Schoepp DD. *J Med Chem*. **2003**; 46: 3189–92.

12. Galici R, Jones CK, Hemstapat K, Nong Y, Echemendia NG, Williams LC, de Paulis T, Conn PJ. *J Pharmacol Exp Ther*. **2006**; 318: 173–85.

13. Fell MJ, Witkin JM, Falcone JF, Katner JS, Perry KW, Hart J, Rorick-Kehn L, Overshiner CD, Rasmussen K, Chaney SF, Benvenga MJ, Li X, Marlow DL, Thompson LK, Luecke SK, Wafford KA, Seidel WF, Edgar DM, Quets AT, Felder CC, Wang X, Heinz BA, Nikolayev A, Kuo M-S, Mayhugh D, Khilevich A, Zhang D, Ebert PJ, Eckstein JA, Ackermann BL, Swanson SP, Catlow JT, Dean RA, Jackson K, Tauscher-Wisniewski S, Marek GJ, Schkeryantz JM, Svensson KA. *J Pharmacol Exp Ther*. **2011**; 336: 165–177.

14. Lavreysen H, Langlois X, Ahnaou A, Drinkenburg W, te Riele P, Biesmans I, Van der Linden I, Peeters L, Megens A, Wintmolders C, Cid JM, Trabanco AA, Andrés JI, Dautzenberg FM, Lütjens R, Macdonald G, Atack JR. *J Pharmacol Exp Ther*. **2013**; 346: 514–27.

15. Ball M, Boyd A, Churchill G, Cuthbert M, Drew M, Fielding M, Ford G, Frodsham L, Golden M, Leslie K, Lyons S, McKeever-Abbas B, Stark A, Tomlin P, Gottschling S, Hajar A, Jiang J, Lo J, Suchozak B. *Org Process Res Dev*. **2012**; 16: 741–747.

16. Cook D, Brown D, Alexander R, March R, Morgan P, Satterthwaite G, Pangalos MN. *Nat Rev Drug Discov*. **2014**; 13: 419–31.

17. Cid JM, Tresadern G, Duvey G, Lütjens R, Finn T, Rocher J, Poli S, Vega JA, de Lucas AI, Matesanz E, Linares ML, Andrés JI, Alcazar J, Alonso JM, Macdonald GJ, Oehlrich D, Lavreysen H, Ahnaou A, Drinkenburg W, Mackie C, Pype S, Gallacher D, Trabanco AA. *J Med Chem*. **2014**; 57: 6495–512.

18. Schaffhauser H, Rowe BA, Morales S, Chavez-Noriega LE, Yin R, Jachec C, Rao SP, Bain G, Pinkerton AB, Vernier J, Bristow LJ, Varney MA, Daggett LP. *Mol Pharmacol*. **2003**; 64: 798–810.

19. Rowe BA, Schaffhauser H, Morales S, Lubbers LS, Bonnefous C, Kamenecka TM, McQuiston J, Daggett LP. *J Pharmacol Exp Ther*. **2008**; 326: 240–51.

20. Hemstapat K, Da Costa H, Nong Y, Brady AE, Luo Q, Niswender CM, Tamagnan GD, Conn PJ. *J Pharmacol Exp Ther*. **2007**; 322: 254–64.

21. Lundström L, Bissantz C, Beck J, Wettstein JG, Woltering TJ, Wichmann J, Gatti S. *Br J Pharmacol*. **2011**; 164: 521–37.

22. Farinha A, Lavreysen H, Peeters L, Russo B, Masure S, Trabanco AA, Cid J, Tresadern G. *Br J Pharmacol*. **2015**; 172: 2383–96.

23. Wu H, Wang C, Gregory KJ, Han GW, Cho HP, Xia Y, Niswender CM, Katritch V, Meiler J, Cherezov V, Conn PJ, Stevens RC. *Science*. **2014**; 344: 58–64.

24. Doré AS, Okrasa K, Patel JC, Serrano-Vega M, Bennett K, Cooke RM, Errey JC, Jazayeri A, Khan S, Tehan B, Weir M, Wiggin GR, Marshall FH. *Nature*. **2014**; 511: 557–62.

25. Woltering TJ, Wichmann J, Goetschi E, Knoflach F, Ballard TM, Huwyler J, Gatti S. *Bioorg Med Chem Lett*. **2010**; 20: 6969–74.

26. Cid-Nuñez, J. M., Oehlrich, D., Trabanco-Suárez, A. A., Tresadern, G. J., Vega Ramiro, J. A., MacDonald, G. J.WO 2010/130424 A1 **2010**.

27. Cuisset L, Tichonicky L, Jaffray P, Delpech M. *J Biol Chem*. **1997**; 272: 24148–24153.

28. Smith PK, Krohn RI, Hermanson GT, Mallia AK, Gartner FH, Provenzano MD, Fujimoto EK, Goeke NM, Olson BJ, Klenk DC. *Anal Biochem*. **1985**; 150: 76–85.

29. Cheng Y, Prusoff WH. *Biochem Pharmacol*. **1973**; 22: 3099–108.

30. Rasmussen SGF, DeVree BT, Zou Y, Kruse AC, Chung KY, Kobilka TS, Thian FS, Chae PS, Pardon E, Calinski D, Mathiesen JM, Shah ST a, Lyons J a, Caffrey M, Gellman SH, Steyaert J, Skiniotis G, Weis WI, Sunahara RK, Kobilka BK. *Nature*. **2011**; 477: 549–55.

31. El Moustaine D, Granier S, Doumazane E, Scholler P, Rahmeh R, Bron P, Mouillac B, Banères J-L, Rondard P, Pin J-P. *Proc Natl Acad Sci U S A*. **2012**; 109: 16342–7.

32. Isberg V, de Graaf C, Bortolato A, Cherezov V, Katritch V, Marshall FH, Mordalski S, Pin J-P, Stevens RC, Vriend G, Gloriam DE. *Trends Pharmacol Sci*. **2015**; 36: 22–31.

33. Cid JM, Tresadern G, Vega JA, de Lucas AI, Matesanz E, Iturrino L, Linares ML, Garcia A, Andrés JI, Macdonald GJ, Oehlrich D, Lavreysen H, Megens A, Ahnaou A, Drinkenburg W, Mackie C, Pype S, Gallacher D, Trabanco AA. *J Med Chem*. **2012**; 55: 8770–89.

34. Hess B, Kutzner C, van der Spoel D, Lindahl E. *J Chem Theory Comput*. **2008**; 4: 435–447.

35. Lindorff-Larsen K, Piana S, Palmo K, Maragakis P, Klepeis JL, Dror RO, Shaw DE. *Proteins*. **2010**; 78: 1950–8.

36. Berger O, Edholm O, Jähnig F. *Biophys J*. **1997**; 72: 2002–13.

37. Cordomí A, Caltabiano G, Pardo L. *J Chem Theory Comput*. **2012**; 8: 948–958.

38. Christopoulos A, Kenakin T. *Pharmacol Rev*. **2002**; 54: 323–74.

39. Lavreysen H, Ahnaou A, Drinkenburg W, Langlois X, Mackie C, Pype S, Lütjens R, Le Poul E, Trabanco AA, Nuñez JMC. *Pharmacol Res Perspect*. **2015**; 3: e00096.

40. Keov P, Sexton PM, Christopoulos A. *Neuropharmacology*. **2011**; 60: 24–35.

41. Gregory KJ, Noetzel MJ, Rook JM, Vinson PN, Stauffer SR, Rodriguez AL, Emmitte K a, Zhou Y, Chun AC, Felts AS, Chauder B a, Lindsley CW, Niswender CM, Conn PJ. *Mol Pharmacol*. **2012**; 82: 860–75.

42. Goudet C, Kniazeff J, Hlavackova V, Malhaire F, Maurel D, Acher F, Blahos J, Prézeau L, Pin J-P. *J Biol Chem*. **2005**; 280: 24380–5.

43. Hlavackova V, Goudet C, Kniazeff J, Zikova A, Maurel D, Vol C, Trojanova J, Prézeau L, Pin J-P, Blahos J. *EMBO J*. **2005**; 24: 499–509.

44. Williams LT, Lefkowitz RJ. *J Biol Chem*. **1977**; 252: 7207–13.

45. Schaffhauser H, Richards JG, Cartmell J, Chaboz S, Kemp JA, Klingelschmidt A, Messer J, Stadler H, Woltering T, Mutel V. *Mol Pharmacol*. **1998**; 53: 228–33.

46. Cartmell J, Adam G, Chaboz S, Henningsen R, Kemp JA, Klingelschmidt A, Metzler V, Monsma F, Schaffhauser H, Wichmann J, Mutel V. *Br J Pharmacol*. **1998**; 123: 497–504.

47. Tresadern G, Cid JM, Macdonald GJ, Vega JA, de Lucas AI, García A, Matesanz E, Linares ML, Oehlrich D, Lavreysen H, Biesmans I, Trabanco AA. *Bioorg Med Chem Lett*. **2010**; 20: 175–9.

48. Deupi X, Standfuss J. *Curr Opin Struct Biol*. **2011**; 21: 541–551.

49. Liu W, Chun E, Thompson A a, Chubukov P, Xu F, Katritch V, Han GW, Roth CB, Heitman LH, IJzerman AP, Cherezov V, Stevens RC. *Science*. **2012**; 337: 232–6.

50. Xue L, Rovira X, Scholler P, Zhao H, Liu J, Pin J-P, Rondard P. *Nat Chem Biol*. **2015**; 11: 134–40.